

# MALDI Investigation of the Photooxidation of Nylon-66

Sabrina Carroccio\* and Concetto Puglisi

*Istituto di Chimica e la Tecnologia dei Polimeri (Sez. Catania), Consiglio Nazionale delle Ricerche, Viale A. Doria, 6-95125 Catania, Italy*

Giorgio Montaudo\*

*Dipartimento di Scienze Chimiche, Università di Catania. Viale A. Doria, 6-95125 Catania, Italy*

*Received March 10, 2004; Revised Manuscript Received May 4, 2004*

**ABSTRACT:** Matrix-assisted laser desorption/ionization mass spectrometry (MALDI) was used to determine the structure of the molecules produced in the photooxidative degradation of nylon-66 at 60 °C in air. The MALDI spectra of the photooxidized nylon-66 (Ny66) show the presence of nearly 40 compounds, as compared to only four in the original Ny66 sample, and provide information on the structure and end groups of the oligomers produced in the oxidation. The structural analysis of the photooxidized species provided by the MALDI spectra allowed drawing a detailed map of the photodecomposition mechanisms of Ny66. Our results extend the currently accepted picture for the photooxidation mechanisms of Ny66, confirming previous insights into the hydrogen abstraction and subsequent formation of a hydroperoxide intermediate, but also reveal that Norrish I and Norrish II chain cleavage reactions play an important role in the photooxidation process of Ny66. Ny66 films exposed for 12 h show the appearance of only photooxidation products generated by the hydrogen peroxide decomposition, indicating that the chain photocleavage reactions Norrish I and Norrish II type do occur at a later stage of irradiation. An explanation is offered for the appearance of this induction period. It is expected that future MALDI studies may have an impact on the current views on photooxidation processes of other polymer systems.

## Introduction

Aliphatic polyamides find wide application as engineering plastics and fiber material, and during their normal use they are exposed to sunlight. Photoaging of this class of polyamides is of greatest concern since many security devices are made with this high-performance material.

The mechanism of photooxidation is crucial for the understanding of natural aging of aliphatic polyamides, and it has been widely studied.<sup>1–10</sup>

Remarkable information on the photooxidation of nylon-66 (Ny66) has been provided in the past by investigations that used mainly UV, IR, and wet chemistry methods to follow the process and to identify the products formed.<sup>1–10</sup>

The hydroperoxides formed in photooxidation of Ny66 have been determined,<sup>9</sup> and chemiluminescence has been used<sup>11</sup> to correlate light emission and rate of oxidation in Ny66.

The main step in photooxidation of Ny66 is believed to consist in a hydrogen abstraction from the methylene group adjacent to the amide NH, leading then to the formation of a hydroperoxide intermediate, which then decomposes thermally, generating the actual products of Ny66 photooxidation, as shown in Scheme 1.<sup>1–10</sup>

However, molecules formed in the photooxidation processes are often very reactive, do not accumulate, and are present only in minor amounts among the reaction products. Conventional analytical techniques as UV and IR might prove inadequate in providing exhaustive information on the molecular structure of the complex mixture of compounds present in the photooxidized Ny66 samples, therefore leaving room for more detailed investigations.

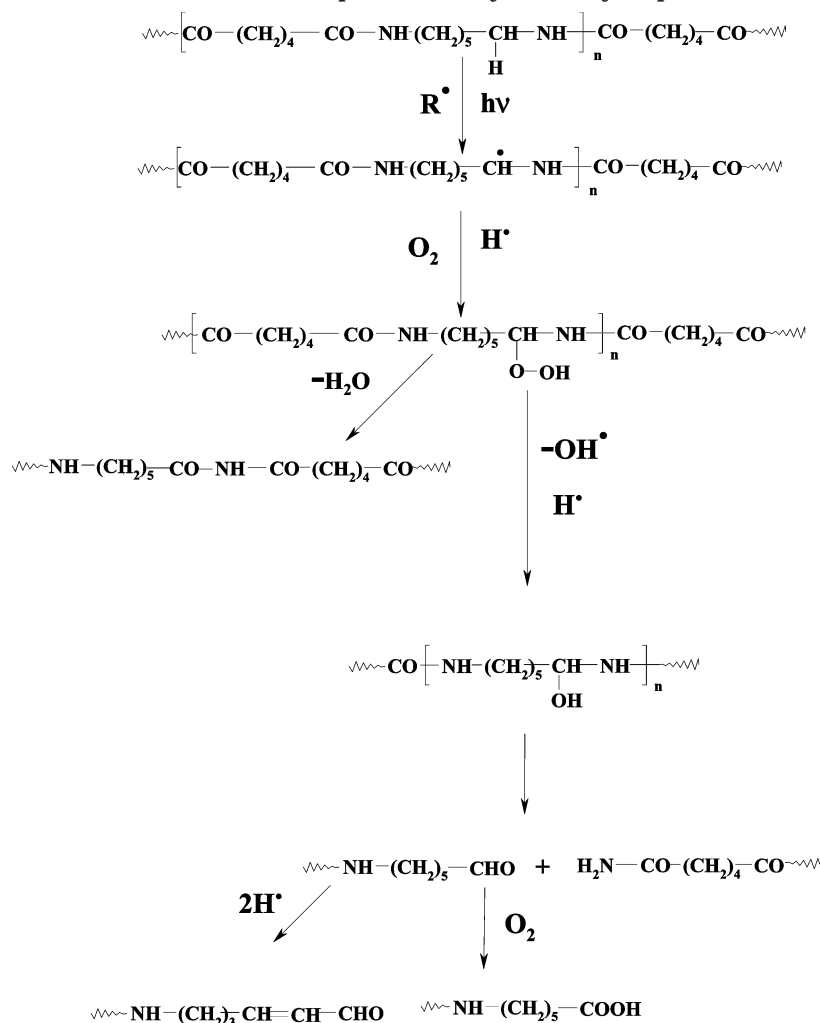
In the past decade the analysis of polymers has taken advantage from the development of the matrix-

assisted laser desorption/ionization–time-of-flight–MS (MALDI), a high-sensitivity, nonaveraging<sup>12</sup> technique that allows the direct determination of the individual species contained in a polymer sample.<sup>13,14</sup>

Applications of MALDI to the study of polymer thermo- and photooxidation are quite recent<sup>15–24</sup> and involve the collection of MALDI spectra at different irradiation times and/or temperature to observe the structural changes induced by heat or light under an oxidizing atmosphere. The polymer sample can be directly analyzed and the recorded MALDI spectrum arises from a mixture of nonoxidized and oxidized chains. MALDI spectra yield precise information on the size, structure, and end groups of molecules that originated in the oxidation process, allowing the discrimination among possible oxidation mechanisms.

In previous work,<sup>24</sup> we have reported on the MALDI characterization of the products formed in Ny66 thermally treated. In the present work Ny66 films were subjected to photoaging, and the photooxidation products were analyzed by MALDI. The spectra thus obtained carry a rich mass of structural information on the products of photooxidation of Ny66, and the new data lead us to speculate about the oxidation mechanisms of nylon-66.

According to the structure of the products identified in the present investigation, three photooxidation processes are occurring in Ny66. Besides the hydrogen abstraction and subsequent hydroperoxide formation, which had been established in previous studies,<sup>1–10</sup> two other major processes appear to be operating in Ny66, i.e., chain cleavage reactions Norrish type I and Norrish type II (Scheme 2). Remarkably, these results come in close agreement with the twin study made on nylon-6, 19,23

**Scheme 1. Photodecomposition of Nylon-66 Hydroperoxides**

## Experimental Section

**Materials.** 2-(4-Hydroxyphenylazo)benzoic acid (HABA) and trifluoroethanol were analytical grade materials, purchased from Sigma-Aldrich Chemical Co. (Italy) and used as supplied. Ny66 ( $M_n = 27\,000$ ) was supplied by Sigma-Aldrich, and it was dried at 80 °C under vacuum for 2 days.

**Photooxidation Procedure.** The photooxidation was performed on films of nylon-66 with a uniform thickness of 10  $\mu\text{m}$ . Films were obtained by casting from 2% trifluoroethanol solution. Photooxidative degradation of nylon-66 films was carried out on a QUV PANEL apparatus at 60 °C with continued exposure to UV radiation up to 147 h. At least two separate films were analyzed at each exposure time. The irradiance of the UV lamps (UVA 340 lamps) has a broad band with a maximum at 340 nm.

**MALDI: Sample Preparation and Analytical Procedures.** The samples for the MALDI analyses were prepared by mixing adequate volumes of the matrix solution (HABA, 0.1 M in TFE) and of polymer solution (2 mg/mL in TFE) to obtain a 1:1 or 1:3 ratio (sample/matrix) v/v. 1  $\mu\text{L}$  of a 0.1 M solution of sodium trifluoroacetate (NaTFA) in TFE was added to aid cationization. 1  $\mu\text{L}$  of each sample/matrix mixture was spotted on the MALDI sample holder and slowly dried to allow matrix crystallization.

Matrix-assisted laser desorption ionization–time-of-flight (MALDI–TOF) mass spectra were obtained using a Voyager-DE STR instrument, equipped with a nitrogen laser emitting a 337 nm with a 3 ns pulse width and working in positive ion mode. The accelerating voltage was 20–25 kV, and the grid voltage and delay time (delayed extraction, time lag) were optimized for each sample to obtain the higher molar mass

values. The laser irradiance was maintained slightly above threshold.

The resolution of the MALDI spectra reported in the text is about 7000 fwhm, and the accuracy of mass determination after external calibration was lower than 220 ppm for masses in the range 928–1800 Da.

To distinguish and separate between the contribution of isotopic peaks  $M + 1$  and  $M + 2$  and peaks due to isobaric structures, a deisotoping program (Mariner Lab) was used. This program produces a theoretical spectrum for each species and subtracts from experimental spectrum the intensity calculates values of  $M + 1$  and  $M + 2$  isotopic peaks. Thus, the deisotoping spectrum shows only the first mass peaks  $M$  for each species.

The structural identification of MALDI peaks in Table 3 was mainly made on the basis of empirical formulas. However, isotopic resolution helps considerably in the peak assignment process through the comparison of the relative intensities of isotopic peaks corresponding to oligomers of increasing molar mass.<sup>17</sup> Some plausible structures were also derived from previous studies.<sup>1–10,18</sup>

As an example, the structure of the  $\alpha,\beta$ -unsaturated aldehydes (Table 3) could have the unsaturation anywhere in the chain, in the absence of corroborating information.<sup>1,3–9</sup> Assignments in Table 3 are therefore strongly suggestive but not absolute.

**Determination of Molar Masses.** Molar mass values were calculated from viscosity measurements. The solution viscosity was measured at  $25 \pm 0.1$  °C with an Ubbelohde viscometer employing concentrations of 0.5 g/dL in a 90% aqueous solution of HCOOH.<sup>26</sup> The Mark–Houwink coef-



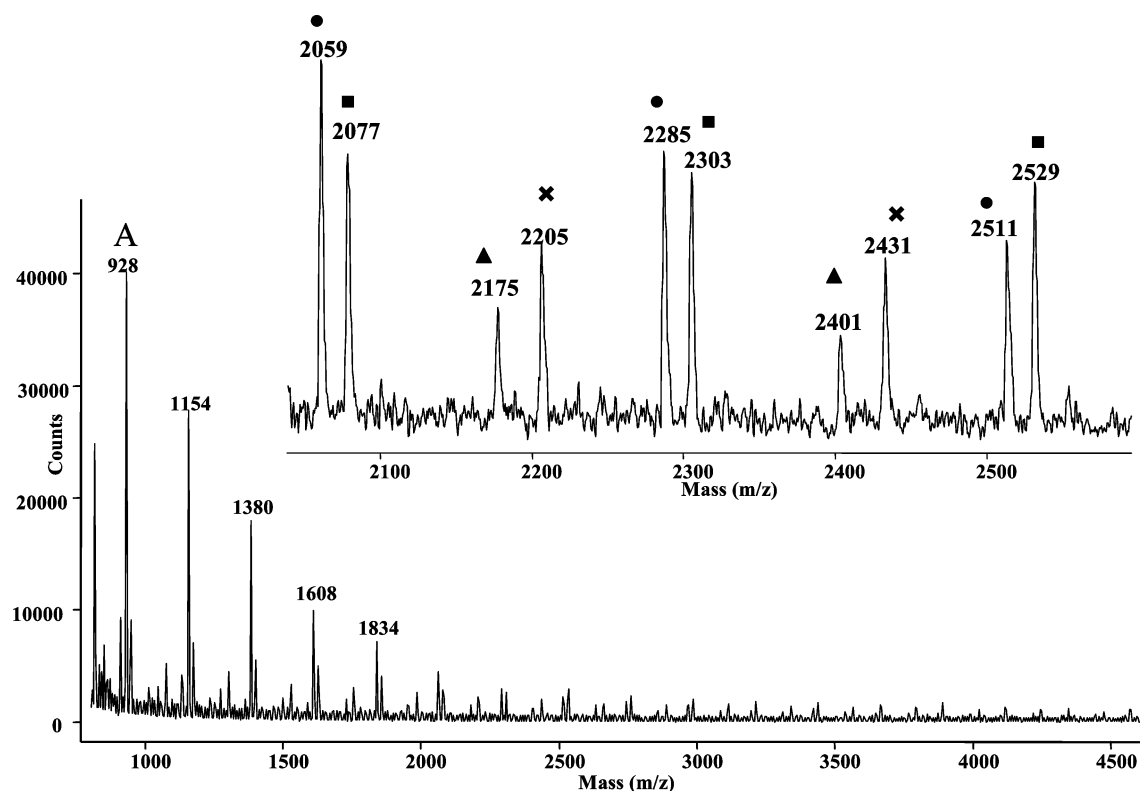


**Figure 1.** MALDI–TOF mass spectrum of Ny66 sample in the mass range 1000–4500 Da obtained in reflectron mode.

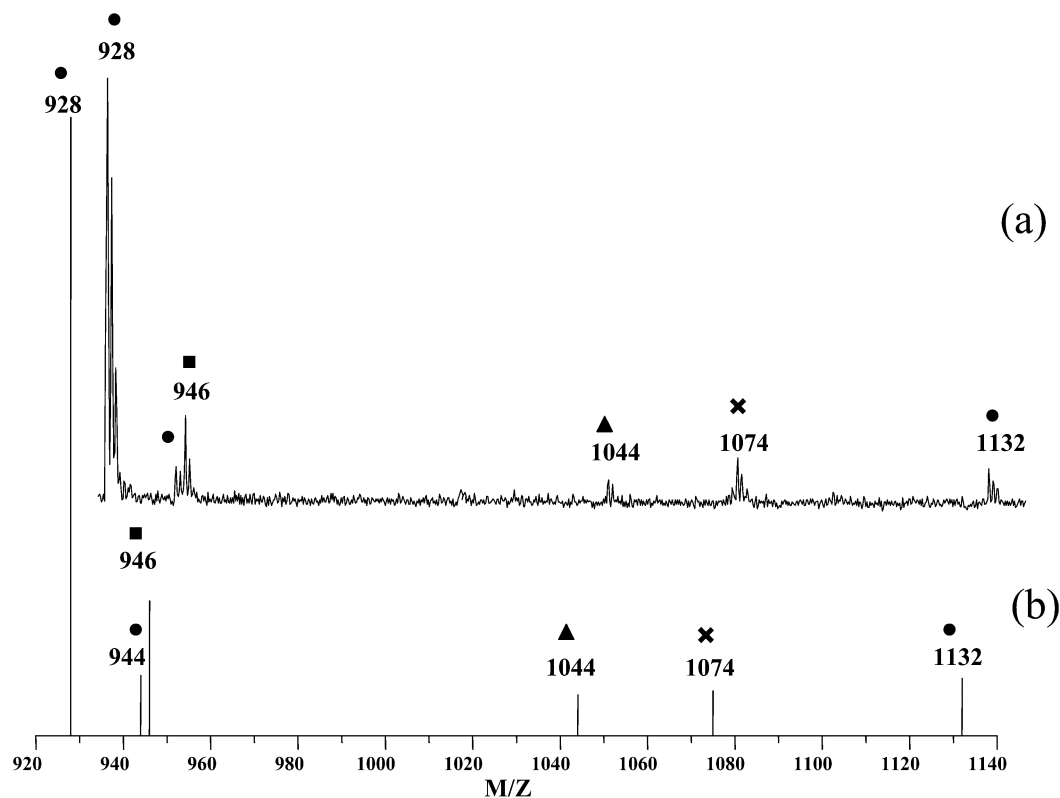


**Figure 2.** (a) Expanded MALDI–TOF mass spectra of Ny66 in the mass range of 920–1140 obtained in reflectron mode; (b) after deisotoping.

The MALDI peaks in Figures 1 and 2 are due to four series of oligomers, which are identified in Table 2: (i) sodiated, pothassiated, and protonated ions of cyclic nylon-66 chains (species ●;  $m/z$  928, 944, and 1032); (ii) sodiated ions of linear oligomers terminated

with carboxyl at one end and with amino groups at the other end (species ■;  $m/z$  946); (iii) sodiated ions of linear oligomers terminated with two amino groups at the ends (species ▲;  $m/z$  1044); (iiii) sodiated ions of linear oligomers terminated with two carbonyl

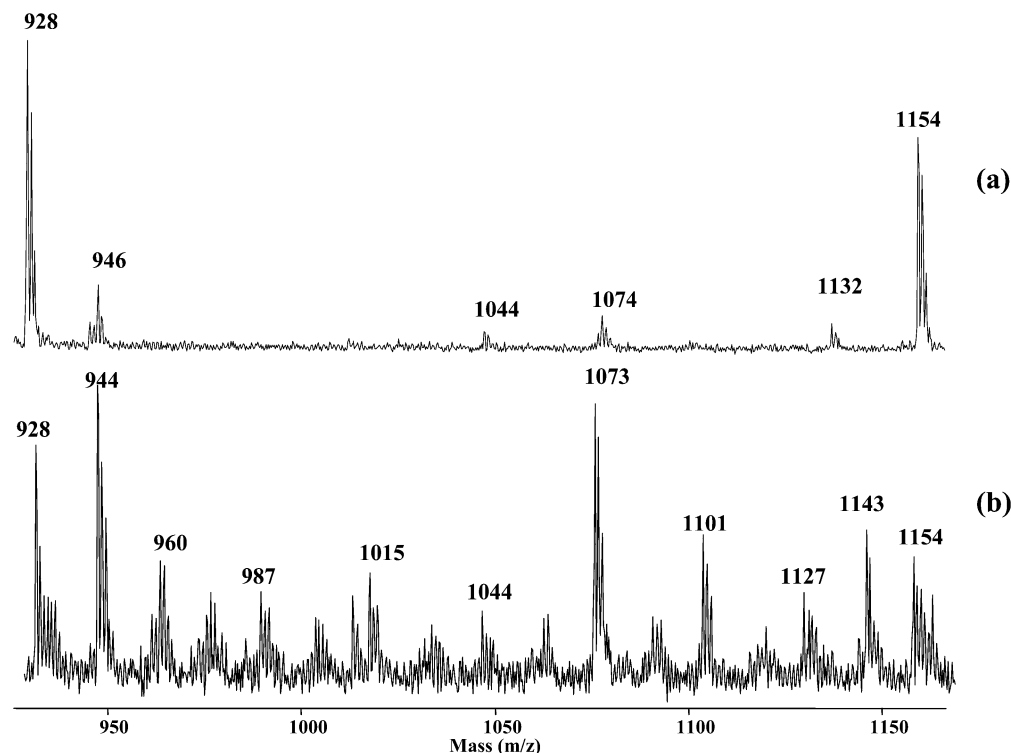


**Figure 3.** Expanded MALDI-TOF mass spectra in the mass range 920–1158 Da of (a) original nylon-66 sample and (b) photooxidized for 147 h.

**Table 2.** Structural Assignments of Ions Appearing in the MALDI-TOF Spectra of Ny66 Sample in Figures 1 and 2

Species	Structures	Mass $H^+$	Mass $Na^+$
●	$\left[ \text{CO}-(\text{CH}_2)_4-\text{CO}-\text{NH}-(\text{CH}_2)_6-\text{NH} \right]_n$	$n=5$ 1132	$n=4$ 928 $n=9$ 2059
■	$\text{HO}-\left[ \text{CO}-(\text{CH}_2)_4-\text{CO}-\text{NH}-(\text{CH}_2)_6-\text{NH} \right]_n-\text{H}$		$n=4$ 946 $n=9$ 2077
▲	$\text{H}-\left[ \text{NH}-(\text{CH}_2)_6-\text{NH}-\text{CO}-(\text{CH}_2)_4-\text{CO} \right]_n-\text{NH}-(\text{CH}_2)_6-\text{NH}_2$		$n=4$ 1044 $n=9$ 2175
×	$\text{HOOC}-(\text{CH}_2)_4-\text{CO}-\left[ \text{NH}-(\text{CH}_2)_6-\text{NH}-\text{CO}-(\text{CH}_2)_4-\text{CO} \right]_n-\text{OH}$		$n=4$ 1074 $n=9$ 2205

groups at the ends (species ×;  $m/z$  1074). The intensity of the cyclic oligomers decreases rapidly at masses beyond 2000, contrary to the intensity of the linear oligomers (Figure 1). Therefore, the Ny66 sample under investigation can be considered mainly constituted of linear chains.

In parts a and b of Figure 3 are reported expanded portions of the MALDI spectra of Ny66 samples irradiated for 0 and 147 h, respectively. For the irradiated sample it is possible to observe a sensible increment of peaks with respect to the original sample in Figure 3a. This indicates that photooxidation reactions have occurred in nylon-66, producing new compounds that are detected and differentiated by the MALDI analysis.

The favorable event here is that the MALDI spectra present so many new well-resolved peaks, which provide

potential information on the structure and end groups of the oxidation products.

Because of the effect of the isotopic resolution, the identity and relative intensity of the peaks in Figure 3b are not easily assessed, and therefore in Figure 4 is shown the spectrum the Ny66 sample irradiated for 72 h after deisotoping.

Nearly 40 peaks are present in the mass spectrum of the oxidized sample, as compared to only four in the original Ny66 sample.

All these peaks correspond to sodiated ions of oxidized Ny66 oligomers, and they have been assigned (Table 3) to specific oligomer structures and to specific oxidation pathways.

The identification of the end groups attached to the oligomers produced in the oxidation process is of out-

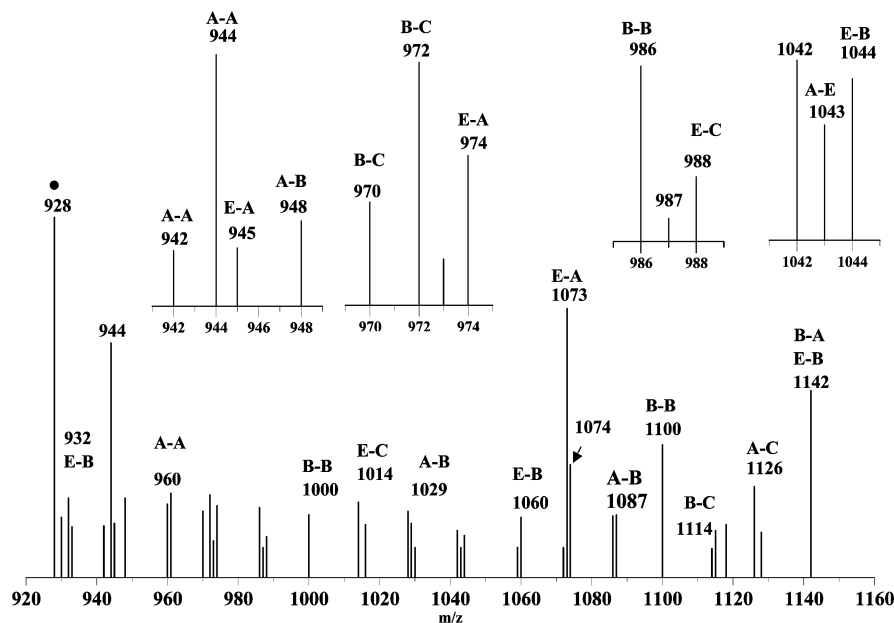
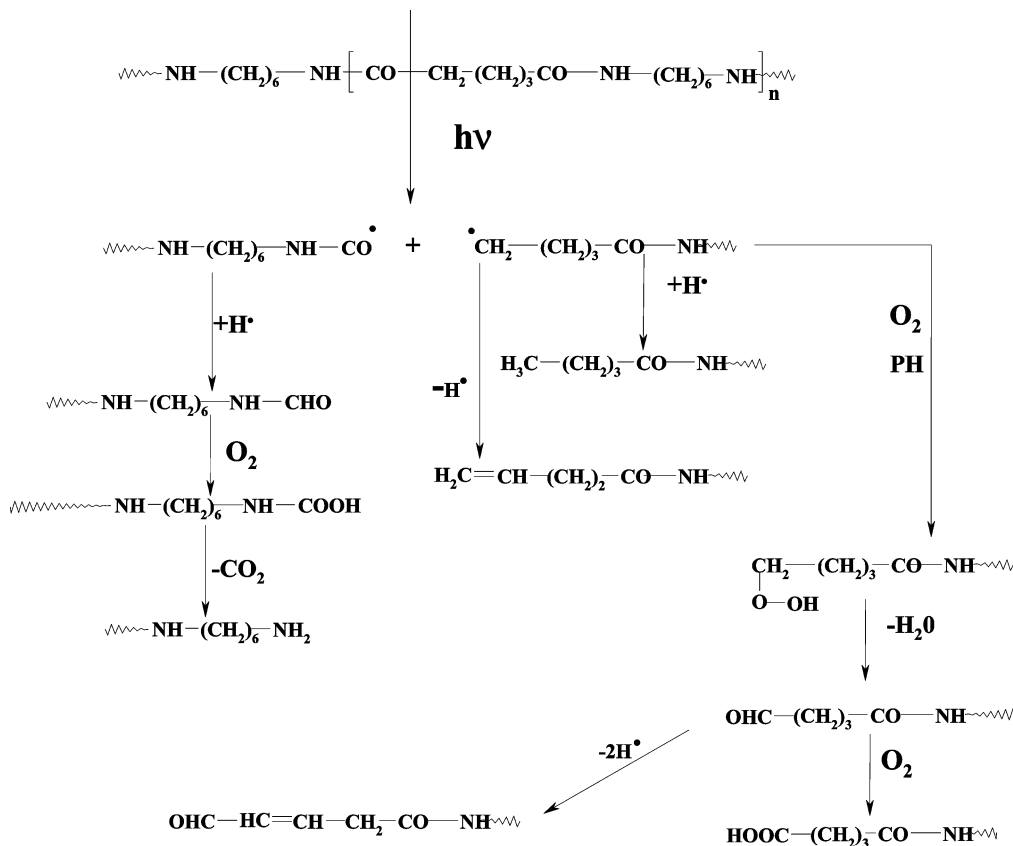


**Figure 4.** Deisotoping MALDI-TOF mass spectrum in the mass range 920–1140 Da of photooxidized nylon-66 sample for 72 h.

**Scheme 3. Photodecomposition of Nylon-66 by Norrish I Reaction**



most importance, since the end groups may reveal the particular mechanism that has been active in the oxidation process.

According to the structure of the major oxidation products identified, three photooxidation processes appear to be simultaneously occurring in Ny66, as summarized in Scheme 2.

Besides the hydrogen abstraction and subsequent hydroperoxide formation, two other processes appear to be operating in Ny66, i.e., the chain cleavage reactions Norrish I and Norrish II type (Scheme 2).

A detailed map of the processes and of the end groups generated by the hydroperoxide decomposition in Ny66 molecules (route A) is given in Scheme 1. The hydroperoxides initially formed undergo thermal degradation to produce imide units inside the chain, plus aldehyde,  $\alpha,\beta$ -unsaturated aldehyde, N-1-hydroxylated, acid, and amide end groups.

Schemes 3 and 4 illustrate the oxidation processes occurring when the chain cleavage is promoted by the well-known reactions Norrish type I and Norrish type II (routes B and C, respectively).

**Table 3. Structural Assignments of Sodiated Ions Appearing in the MALDI-TOF Spectra of Photooxidized Ny66 Samples in Figures 3–5**

Photo-oxidation processes <sup>a)</sup>	Structures	MNa <sup>+</sup>
C-C	$\text{CH}_3\text{-CO}\left[\text{NH-(CH}_2\text{)}_6\text{-NH-CO-(CH}_2\text{)}_4\text{-CO}\right]_3\text{NH-(CH}_2\text{)}_6\text{-NH-CO-CH}_2\text{-CH=CH}_2$	928
B-B	$\text{OHC-NH-(CH}_2\text{)}_6\text{-NH}\left[\text{CO-(CH}_2\text{)}_4\text{-CO-NH-(CH}_2\text{)}_6\text{-NH}\right]_3\text{CO-(CH}_2\text{)}_3\text{CH}_3$	930
A-B	$\text{OHC-(CH}_2\text{)}_3\text{-CO}\left[\text{NH-(CH}_2\text{)}_6\text{-NH-CO-(CH}_2\text{)}_4\text{-CO}\right]_3\text{NH-(CH}_2\text{)}_5\text{COOH}$	932
E-A	$\left[\text{CO-(CH}_2\text{)}_4\text{-CO-NH-(CH}_2\text{)}_6\text{-NH}\right]_3\text{CO-(CH}_2\text{)}_4\text{-CO-NH-CO-(CH}_2\text{)}_5\text{NH}$	942
A-A	$\text{H}_2\text{NOC-(CH}_2\text{)}_4\text{-CO}\left[\text{NH-(CH}_2\text{)}_6\text{-NH-CO-(CH}_2\text{)}_4\text{-CO}\right]_3\text{NH-(CH}_2\text{)}_3\text{-CH=CH-CHO}$	942
B-C	$\text{H}_3\text{C-(CH}_2\text{)}_3\text{-CO-NH-(CH}_2\text{)}_6\text{-NH}\left[\text{CO-(CH}_2\text{)}_4\text{-CO-NH-(CH}_2\text{)}_6\text{-NH}\right]_3\text{COCH}_3$	944
A-A	$\text{H}_2\text{NOC-(CH}_2\text{)}_4\text{-CO}\left[\text{NH-(CH}_2\text{)}_6\text{-NH-CO-(CH}_2\text{)}_4\text{-CO}\right]_3\text{NH-(CH}_2\text{)}_5\text{-CHO}$	944
B-B	$\text{OHC-(CH}_2\text{)}_3\text{-CO-NH-(CH}_2\text{)}_6\text{-NH}\left[\text{CO-(CH}_2\text{)}_4\text{-CO-NH-(CH}_2\text{)}_6\text{-NH}\right]_3\text{CHO}$	944
E-A	$\text{H}\left[\text{NH-(CH}_2\text{)}_6\text{-NH-CO-(CH}_2\text{)}_4\text{-CO}\right]_4\text{NH}_2$	945
E-A	$\text{HOOC-(CH}_2\text{)}_4\text{-CO}\left[\text{NH-(CH}_2\text{)}_6\text{-NH-CO-(CH}_2\text{)}_4\text{-CO}\right]_3\text{NH-(CH}_2\text{)}_5\text{-CHO}$	945
A-B	$\text{HOOC-(CH}_2\text{)}_3\text{-CO}\left[\text{NH-(CH}_2\text{)}_6\text{-NH-CO-(CH}_2\text{)}_4\text{-CO}\right]_3\text{NH-(CH}_2\text{)}_5\text{COOH}$	947
B-A-C	$\text{H}_3\text{C-(CH}_2\text{)}_3\text{-CO-NH-(CH}_2\text{)}_5\text{-CO-NH}\left[\text{CO-(CH}_2\text{)}_4\text{-CO-NH-(CH}_2\text{)}_6\text{-NH}\right]_3\text{COCH}_3$	958
B-B	$\text{HOOC-(CH}_2\text{)}_3\text{-CO-NH-(CH}_2\text{)}_6\text{-NH}\left[\text{CO-(CH}_2\text{)}_4\text{-CO-NH-(CH}_2\text{)}_6\text{-NH}\right]_3\text{CHO}$	960
E-A-C	$\text{HOOC-(CH}_2\text{)}_4\text{-CO}\left[\text{NH-(CH}_2\text{)}_6\text{-NH-CO-(CH}_2\text{)}_4\text{-CO}\right]_3\text{NH-CO-(CH}_2\text{)}_5\text{-NH}_2$	960
A-A	$\text{H}_2\text{NOC-(CH}_2\text{)}_4\text{-CO}\left[\text{NH-(CH}_2\text{)}_6\text{-NH-CO-(CH}_2\text{)}_4\text{-CO}\right]_3\text{NH-(CH}_2\text{)}_5\text{COOH}$	960
E-A	$\text{HOOC-(CH}_2\text{)}_4\text{-CO}\left[\text{NH-(CH}_2\text{)}_6\text{-NH-CO-(CH}_2\text{)}_4\text{-CO}\right]_3\text{NH-(CH}_2\text{)}_5\text{COOH}$	961



Table 3. (Continued)

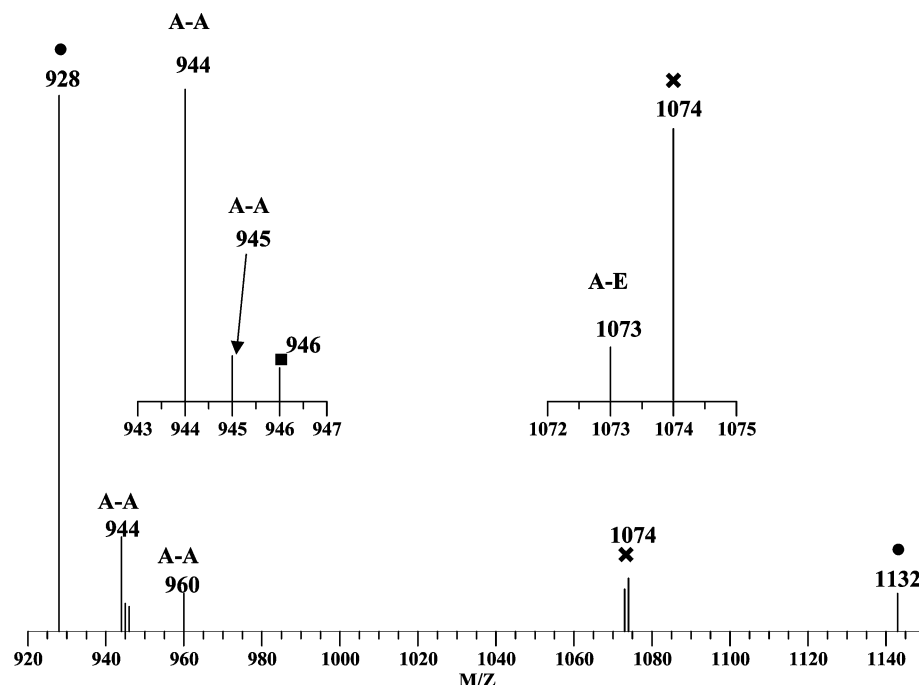
Photo-oxidation processes <sup>a)</sup>	Structures	MNa+
B-C	$\text{H}_3\text{C}-(\text{CH}_2)_3-\text{CO}-\text{NH}-(\text{CH}_2)_6-\text{NH}-\left[\text{CO}-(\text{CH}_2)_4-\text{CO}-\text{NH}-(\text{CH}_2)_6-\text{NH}\right]_3-\text{CO}-\text{CH}_2-\text{CH}=\text{CH}_2$	970
B-C	$\text{H}_3\text{C}-(\text{CH}_2)_3-\text{CO}-\text{NH}-(\text{CH}_2)_6-\text{NH}-\left[\text{CO}-(\text{CH}_2)_4-\text{CO}-\text{NH}-(\text{CH}_2)_6-\text{NH}\right]_3-\text{CO}-(\text{CH}_2)_2-\text{CH}_3$	972
A-B	$\text{H}_2\text{N}-\left[\text{CO}-(\text{CH}_2)_4-\text{CO}-\text{NH}-(\text{CH}_2)_6-\text{NH}\right]_4-\text{CHO}$	973
E-B	$\text{HO}-\left[\text{CO}-(\text{CH}_2)_4-\text{CO}-\text{NH}-(\text{CH}_2)_6-\text{NH}\right]_4-\text{CHO}$	974
B-C	$\text{HOOC}-(\text{CH}_2)_3-\text{CO}-\text{NH}-(\text{CH}_2)_6-\text{NH}-\left[\text{CO}-(\text{CH}_2)_4-\text{CO}-\text{NH}-(\text{CH}_2)_6-\text{NH}\right]_3-\text{COCH}_3$	974
B-B	$\text{H}_3\text{C}-(\text{CH}_2)_3-\text{OC}-\text{NH}-(\text{CH}_2)_6-\text{NH}-\left[\text{CO}-(\text{CH}_2)_4-\text{CO}-\text{NH}-(\text{CH}_2)_6-\text{NH}\right]_3-\text{CO}-(\text{CH}_2)_3-\text{CH}_3$	986
C-A	$\text{CH}_3-\text{CO}-\left[\text{NH}-(\text{CH}_2)_6-\text{NH}-\text{CO}-(\text{CH}_2)_4-\text{CO}\right]_3-\text{NH}_2$	987
E-C	$\text{HO}-\left[\text{CO}-(\text{CH}_2)_4-\text{CO}-\text{NH}-(\text{CH}_2)_6-\text{NH}\right]_4-\text{CO}-\text{CH}_3$	988
B-B	$\text{OHC}-(\text{CH}_2)_3-\text{CO}-\text{NH}-(\text{CH}_2)_6-\text{NH}-\left[\text{CO}-(\text{CH}_2)_4-\text{CO}-\text{NH}-(\text{CH}_2)_6-\text{NH}\right]_3-\text{CO}-(\text{CH}_2)_3-\text{CH}_3$	1000
E-C	$\text{CH}_2=\text{CH}-\text{CH}_2-\text{CO}-\left[\text{NH}-(\text{CH}_2)_6-\text{NH}-\text{CO}-(\text{CH}_2)_4-\text{CO}\right]_4-\text{OH}$	1014
E-C	$\text{H}_3\text{C}-(\text{CH}_2)_2-\text{CO}-\left[\text{NH}-(\text{CH}_2)_6-\text{NH}-\text{CO}-(\text{CH}_2)_4-\text{CO}\right]_4-\text{OH}$	1016
B-B	$\text{HOOC}-(\text{CH}_2)_3-\text{CO}-\text{NH}-(\text{CH}_2)_6-\text{NH}-\left[\text{CO}-(\text{CH}_2)_4-\text{CO}-\text{NH}-(\text{CH}_2)_6-\text{NH}\right]_3-\text{CO}-(\text{CH}_2)_3-\text{CH}_3$	1016
E-B	$\text{HO}-\left[\text{CO}-(\text{CH}_2)_4-\text{CO}-\text{NH}-(\text{CH}_2)_6-\text{NH}\right]_4-\text{CO}-(\text{CH}_2)_2-\text{CH}=\text{CH}_2$	1028
A-B	$\text{H}_2\text{N}-\left[\text{CO}-(\text{CH}_2)_4-\text{CO}-\text{NH}-(\text{CH}_2)_6-\text{NH}\right]_4-\text{CO}-(\text{CH}_2)_3-\text{CH}_3$	1029
E-B	$\text{HO}-\left[\text{CO}-(\text{CH}_2)_4-\text{CO}-\text{NH}-(\text{CH}_2)_6-\text{NH}\right]_4-\text{CO}-(\text{CH}_2)_3-\text{CH}_3$	1030
E-B	$\text{HO}-\left[\text{CO}-(\text{CH}_2)_4-\text{CO}-\text{NH}-(\text{CH}_2)_6-\text{NH}\right]_4-\text{CO}-\text{CH}_2-\text{CH}=\text{CH}-\text{CHO}$	1042
A-E	$\text{OHC}-(\text{CH}_2)_5-\text{NH}-\left[\text{CO}-(\text{CH}_2)_4-\text{CO}-\text{NH}-(\text{CH}_2)_6-\text{NH}\right]_4-\text{H}$	1043
A-B	$\text{H}_2\text{N}-\left[\text{CO}-(\text{CH}_2)_4-\text{CO}-\text{NH}-(\text{CH}_2)_6-\text{NH}\right]_4-\text{CO}-(\text{CH}_2)_3-\text{CHO}$	1043



Table 3. (Continued)

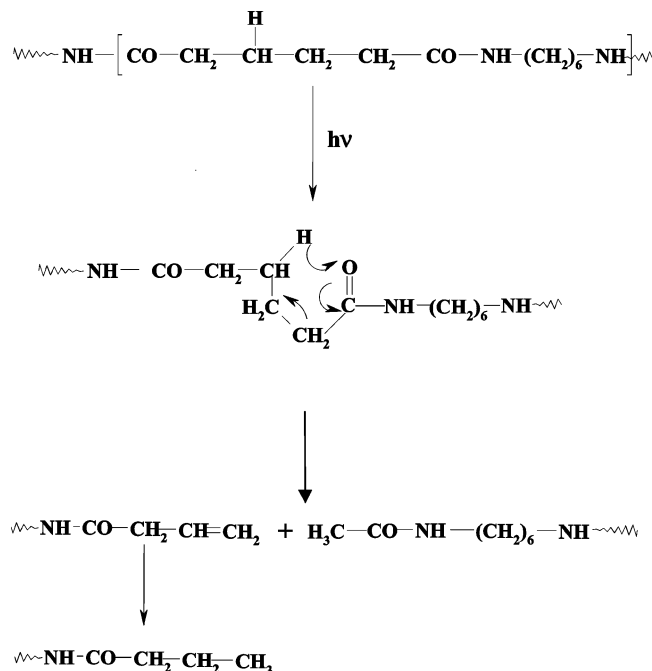
Photo-oxidation processes <sup>a)</sup>	Structures	MNa+
A-A	$\text{OHC}-(\text{CH}_2)_5-\text{HNOC}-(\text{CH}_2)_4-\text{CO}-\left[\text{NH}-(\text{CH}_2)_6-\text{NH}-\text{CO}-(\text{CH}_2)_4-\text{CO}\right]_3-\text{NH}-(\text{CH}_2)_5-\text{CHO}$	1044
E-B	$\text{HO}-\left[\text{CO}-(\text{CH}_2)_4-\text{CO}-\text{NH}-(\text{CH}_2)_6-\text{NH}\right]_4-\text{CO}-(\text{CH}_2)_3-\text{CHO}$	1044
E-A	$\text{H}-\left[\text{NH}-(\text{CH}_2)_6-\text{NH}-\text{CO}-(\text{CH}_2)_4-\text{CO}\right]_4-\text{NH}-(\text{CH}_2)_5-\text{COOH}$	1059
E-B	$\text{H}_2\text{N}-\left[\text{CO}-(\text{CH}_2)_4-\text{CO}-\text{NH}-(\text{CH}_2)_6-\text{NH}\right]_4-\text{CO}-(\text{CH}_2)_3-\text{COOH}$	1059
E-B	$\text{HO}-\left[\text{CO}-(\text{CH}_2)_4-\text{CO}-\text{NH}-(\text{CH}_2)_6-\text{NH}\right]_4-\text{CO}-(\text{CH}_2)_3-\text{COOH}$	1060
A-A	$\text{NH}_2-\text{CO}-(\text{CH}_2)_4-\text{CO}-\left[\text{NH}-(\text{CH}_2)_6-\text{NH}-\text{CO}-(\text{CH}_2)_4-\text{CO}\right]_4-\text{NH}_2$	1072
E-B	$\text{H}_2\text{N}-(\text{CH}_2)_6-\text{NH}-\left[\text{CO}-(\text{CH}_2)_4-\text{CO}-\text{NH}-(\text{CH}_2)_6-\text{NH}\right]_4-\text{CHO}$	1072
A-E	$\text{NH}_2-\text{CO}-(\text{CH}_2)_4-\text{CO}-\left[\text{NH}-(\text{CH}_2)_6-\text{NH}-\text{CO}-(\text{CH}_2)_4-\text{CO}\right]_4-\text{OH}$	1073
E-C	$\text{H}_2\text{N}-(\text{CH}_2)_6-\text{NH}-\left[\text{CO}-(\text{CH}_2)_4-\text{CO}-\text{NH}-(\text{CH}_2)_6-\text{NH}\right]_4-\text{CO}-\text{CH}_3$	1086
B-A	$\text{HOOC}-(\text{CH}_2)_5-\text{NH}-\left[\text{CO}-(\text{CH}_2)_4-\text{CO}-\text{NH}-(\text{CH}_2)_6-\text{NH}\right]_4-\text{CHO}$	1087
B-B	$\text{OHC}-\text{NH}-(\text{CH}_2)_6-\text{NH}-\left[\text{CO}-(\text{CH}_2)_4-\text{CO}-\text{NH}-(\text{CH}_2)_6-\text{NH}\right]_4-\text{CHO}$	1100
B-C	$\text{OHC}-\text{NH}-(\text{CH}_2)_6-\text{NH}-\left[\text{CO}-(\text{CH}_2)_4-\text{CO}-\text{NH}-(\text{CH}_2)_6-\text{NH}\right]_4-\text{COCH}_3$	1114
C-A	$\text{H}_2\text{N}-\text{CO}-(\text{CH}_2)_5-\text{NH}-\left[\text{CO}-(\text{CH}_2)_4-\text{CO}-\text{NH}-(\text{CH}_2)_6-\text{NH}\right]_4-\text{CO}-\text{CH}_2-\text{CH}=\text{CH}_2$	1126
B-E	$\text{CH}_3-(\text{CH}_2)_3-\text{CO}-\left[\text{NH}-(\text{CH}_2)_6-\text{NH}-\text{CO}-(\text{CH}_2)_4-\text{CO}\right]_4-\text{NH}-(\text{CH}_2)_6-\text{NH}_2$	1128
C-C	$\text{CH}_3-\text{CO}-\left[\text{NH}-(\text{CH}_2)_6-\text{NH}-\text{CO}-(\text{CH}_2)_4-\text{CO}\right]_4-\text{NH}-(\text{CH}_2)_6-\text{NH}-\text{CO}-\text{CH}_3$	1128
C-A	$\text{H}_2\text{N}-\text{CO}-(\text{CH}_2)_5-\text{NH}-\left[\text{CO}-(\text{CH}_2)_4-\text{CO}-\text{NH}-(\text{CH}_2)_6-\text{NH}\right]_4-\text{CO}-(\text{CH}_2)_3-\text{CH}_3$	1128
C-C	$\text{CH}_3-\text{CO}-\left[\text{NH}-(\text{CH}_2)_6-\text{NH}-\text{CO}-(\text{CH}_2)_4-\text{CO}\right]_3-\text{NH}-(\text{CH}_2)_6-\text{NH}-\text{CO}-(\text{CH}_2)_3-\text{CH}_3$	1128
E-B	$\text{H}_2\text{N}-(\text{CH}_2)_6-\text{NH}-\left[\text{CO}-(\text{CH}_2)_4-\text{CO}-\text{NH}-(\text{CH}_2)_6-\text{NH}\right]_4-\text{CO}-(\text{CH}_2)_3-\text{CHO}$	1142

<sup>a)</sup> Terminal groups originated by specific photooxidation processes: A = hydroperoxides, B = Norrish I, C = Norrish II, and E = end groups of the unexposed nylon-66.



**Figure 5.** Deisotoping MALDI-TOF mass spectrum in the mass range 920–1140 Da of photooxidized nylon-66 sample for 12 h.

**Scheme 4. Photodecomposition of Nylon-66 by Norrish II Reaction**



Norrish type I cleavage reaction (route B) yields amine, alkyl, alkene, aldehyde, acid,  $\alpha,\beta$ -unsaturated aldehyde, and N-formamide end groups (Scheme 3).

Norrish type II reaction (route C) yields acetylamino ( $-\text{NH}-\text{CO}-\text{CH}_3$ ), butylene, and butane end groups (Scheme 4).

In Table 3 are specified the photooxidation mechanisms responsible for the formation of each new oligomer. We have adopted a particular code in order to specify the relationship between each oligomer end group and the photooxidation mechanism from which it is originated.

Thus, the capital letter A (Table 3) specifies any end group generated by the decomposition of the hydroperoxides (Scheme 1); B specifies any end group generated

by the Norrish type I chain cleavage (Scheme 3); C specifies any end group generated by the Norrish type II chain cleavage (Scheme 4), whereas E indicates just one of the end groups present in the original Ny66 sample.

Since each oligomer has two ends, the notation B–A, for instance, means that a Norrish type I chain cleavage occurred at one end and that hydroperoxide decomposition occurred at the other end. Moreover, three letters label some oligomers in Table 3 (for instance: B–A–C, peak at  $m/z$  958). The external letters B and C retain the above meaning, whereas the intermediate letter A means that along the oligomer chain a further oxidation step has occurred, leading to the formation of an imide group (Scheme 1), without chain scission.

The inspection of the spectrum in Figure 4 reveals that the cyclic oligomer at  $m/z$  928 Da, which belongs to the original Ny66 sample, is still present in the photooxidized sample, although it could also be assigned to a photooxidation product generated by Norrish II reaction (Table 3).

The most prominent peak appearing in Figure 4 ( $m/z$  1073 Da) was unequivocally assigned to oligomers with adipic acid at one end and the amide group at the other end (Table 3) generated by the decomposition of the hydroperoxides (Scheme 1).

Also, the peaks at  $m/z$  942, 945, 961 (Table 3) correspond to oligomers generated by the decomposition of the hydroperoxides and consequent cleavage of the original Ny66 sample (Scheme 1).

These oligomers are called here primary products of photooxidation, since they retain one of the end groups existing in the original Ny66 sample and have therefore a strong diagnostic value in assigning a major role to the hydroperoxide cleavage mechanism.

Peaks appearing in the spectrum in Figure 4 at  $m/z$  930, 1000, 1028, 1030, 1042, 1060, 1100, and 1142 belong to oligomers unequivocally generated via Norrish I chain cleavage (Scheme 3). At one chain end, the oligomers at 1028, 1030, and 1060 Da retain the original end group present in the Ny66 chain prior to photo-

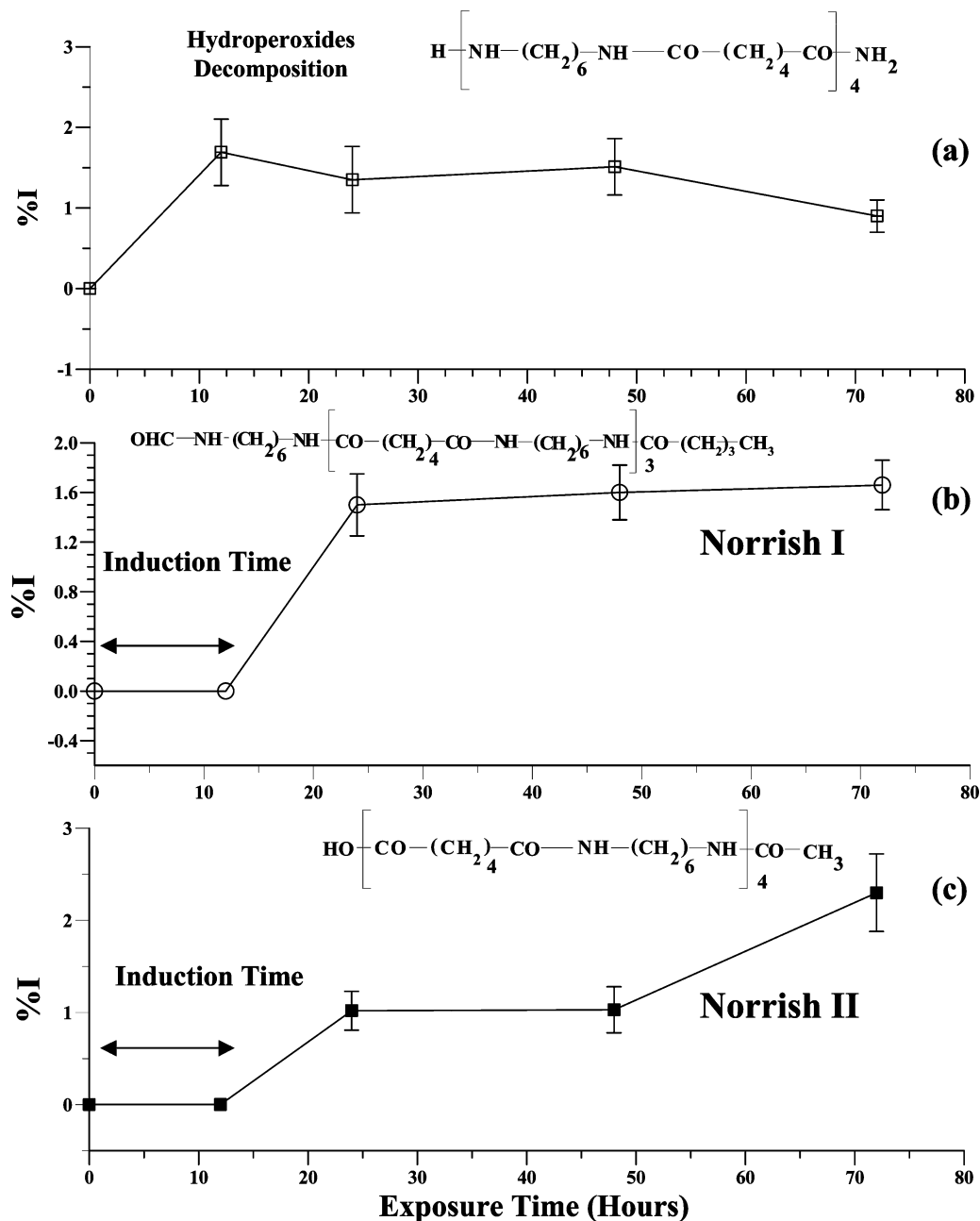


**Figure 6.** Relative amount vs exposure time of species (a) at  $m/z$  945, (b) at  $m/z$  930, and (c) at  $m/z$  988, as obtained from the MALDI spectra of photooxidized nylon-66 sample.

oxidation; thus, they can be assigned to primary photooxidation products.

Finally, peaks at  $m/z$  988, 1014, and 1086 have been unequivocally assigned to primary photooxidation products, generated by a single Norrish type II chain cleavage of the original Ny66 sample (Scheme 4).

The remaining peaks in Figure 4 were assigned to oligomers (Table 3) generated by two (and sometimes three) steps of chain oxidation. These oligomers do not retain end groups existing in the original Ny66 sample and are therefore called secondary photooxidation products.

Going into more details, 10 peaks in Table 3 have been assigned to two or more isobar structures. For instance, the intense peak at  $m/z$  960 (Table 3) has a mass number that may correspond to three isobar structures: a macromolecular ion bearing adipic acid

and amino end groups with an imide unit inside the chain and/or an oligomer with amide end group at one end and caproic acid end group at the other end and/or macromolecular chain having acid group at one end and formamide end group at the other end. This procedure leaves a degree of uncertainty about the mechanisms responsible for the formation of these specific oligomers and constitutes a limit of the present MALDI investigation.

MALDI provides only semiquantitative information as far as peak intensity data are concerned;<sup>14</sup> therefore, the importance of the three photooxidation mechanisms cannot be deduced directly from the relative intensity of the peaks in Figure 4. However, Norrish type I and hydroperoxide formation photooxidation mechanisms appear to be more important over the Norrish type II process.

The presence of end groups due to Norrish I and Norrish II reactions escaped previous investigations,<sup>1–9</sup> perhaps because the photooxidation products deriving from these processes bear aldehyde (1100 *m/z*), alkyl (1030 *m/z*), and carboxyl end groups (1060 *m/z*); all compounds originated also by the hydroperoxide decomposition (Scheme 2, Table 3).

Assignments based on the simple detection of functional end groups (as those provided by IR and UV methods)<sup>1–9</sup> can be only tentative, since functional groups carry no information on the entire structure of the oligomers formed in the oxidation processes. The latter instead is provided by the MALDI data.

Our results also provide insight into the product distribution changes during the photooxidation reaction.

In Figure 5 is reported the MALDI spectrum of a Ny66 film exposed for only 12 h, which shows the appearance of only a few photooxidation products, all of which generated (Table 3) by the hydrogen peroxide decomposition (process A, Scheme 1).

This indicates that the chain photocleavage reactions of Norrish I and Norrish II type do occur at a later stage of irradiation.<sup>25</sup>

In Figure 6a–c are reported the kinetic tracings of the oxidation products, representative of the three oxidation mechanisms found to be operating. The photo-products originating from Norrish I and Norrish II reactions do appear after an induction period, whereas the oligomer generated by the hydrogen peroxide decomposition is formed immediately.

The detection of an induction period before the occurrence of Norrish I and II reactions is a recent (and unexpected) discovery made during the MALDI analysis of Ny6 photooxidation processes,<sup>19</sup> now confirmed for Ny66, and also in the case of the photooxidation of aliphatic polyesters.<sup>20</sup>

A tentative explanation of this phenomenon is offered here. The initial irradiation of these polymers triggers the  $\alpha$ -hydrogen abstraction, a low-energy process in Nylons, which induces the polymer oxidation through the formation of the hydroperoxides. The latter are thermally unstable at 60 °C and decompose, forming oligomers with functional end groups that enhance the light absorption power of the oxidized polymer.

The UV absorption of the unexposed Ny66 films shows a weak maximum at about 225 nm, but the UV absorption dramatically increases and widens toward the longer wavelengths with the exposure time,<sup>9</sup> most likely due to the presence of the photooxidation products. The higher amount of light available to the films absorption induces a sensible increment on the rate of cleavage of C–C bonds and allows the occurrence of the Norrish type processes. This simple two-step model appears to justify the induction periods observed.

## Conclusions

Summarizing our results, a relevant amount of valuable structural information on the photooxidation products of Ny66 has been extracted from the MALDI spectra reported in Figures 1–5.

The peculiarity of our approach consists of using a sensitive and selective technique (mass spectrometry), which allows monitoring the fate of each oligomer during the oxidation process and the detection of many hitherto unidentified products formed in the photo-oxidative degradation of nylon-66.

The data collected show that the photooxidation degradation processes produce a sensible reduction of the molar mass of Ny66 and indicate the formation of Ny66 oligomers with different end groups, consequent to chain cleavage due to oxidation.

The structural identification of the photooxidation products provided by the MALDI spectra allowed drawing a detailed map of the photooxidation mechanisms of Ny66 (Schemes 1–4).

Our results extend the currently accepted picture for the photooxidation mechanisms of Ny66. Our results confirm that the hydrogen abstraction and subsequent formation of a hydroperoxide intermediate actually occurs, but also reveal that Norrish I and Norrish II chain cleavage reactions play an important role in the photooxidation process of Ny66. This essential feature had escaped previous studies.

Ny66 films exposed for 12 h show the appearance of only photooxidation products generated by the hydrogen peroxide decomposition (Scheme 1), indicating that the chain photocleavage reactions Norrish I and Norrish II type do occur at a later stage of irradiation. An explanation has been offered for the appearance of this induction period.

Overall, a remarkable advance has been provided by the present investigation, and it should be expected that future MALDI studies might have an impact on the current views on photooxidation processes of other polymer systems.

**Acknowledgment.** Financial support from the National Council of Research (CNR, Rome) is gratefully acknowledged. The active collaboration of Dr. Giuseppina Scaltro to this work is acknowledged. Many thanks are due to Ms. R. Rapisardi and G. Pastorelli for their continuous and skillful technical assistance.

## References and Notes

- (1) Sharkey, W. H.; Mochel, W. E. *J. Am. Chem. Soc.* **1959**, *81*, 3000–3005.
- (2) Fautitano, A.; Buttafava, A.; Camino, G.; Greci, L. *Trends Polym. Sci.* **1996**, *4*, 92–98.
- (3) Allen, N. S.; McKellar, J. F.; Wilson, D. *J. Photochem.* **1976**, *77*, 337–348.
- (4) Allen, N. S.; Parkinson, A. *Polym. Degrad. Stab.* **1982**, *4*, 239–244.
- (5) Allen, N. S. *Polym. Degrad. Stab.* **1984**, *8*, 55–62.
- (6) Allen, N. S.; Harrison, M. J. *Eur. Polym. J.* **1985**, *21*, 517–526.
- (7) Allen, N. S.; Harrison, M. J.; Follows, G. W.; Matthews, V. *Polym. Degrad. Stab.* **1987**, *19*, 77–95.
- (8) Allen, N. S.; Harrison, M. J.; Follows, G. W.; Matthews, V. *Polym. Degrad. Stab.* **1988**, *21*, 251–262.
- (9) Thanki, P. N.; Singh, R. P. *Polymer* **1998**, *39*, 6363–6367.
- (10) Thanki, P. N.; Singh, R. P. *Polym. Degrad. Stab.* **2002**, *75*, 423–430.
- (11) Cerruti, P.; Carfagna, C.; Rychlý, J.; Matisová-Rychlá, L. *Polym. Degrad. Stab.* **2003**, *82*, 477–485.
- (12) A referee asked to define what is meant saying that MS is a nonaveraging technique. NMR, for instance, is an averaging technique. In NMR spectra all the oligomers having the same chemical structure and end group yield the same resonance peaks, independent of size. Mass spectra, instead, reveal each oligomers present separately, with a specific mass number. A thorough discussion of the consequences can be found in ref 14.
- (13) Hanton, S. D. *Chem. Rev.* **2001**, *101*, 527–569.
- (14) Samperi, F.; Montaudo, M. S.; Montaudo, G. In *Mass Spectrometry of Polymers*; Montaudo, G., Lattimer, R. P., Eds.; CRC Press: Boca Raton, FL, 2001.
- (15) Puglisi, C.; Samperi, F.; Carroccio, S.; Montaudo, G. *Macromolecules* **1999**, *32*, 8821–8828.

- (16) Puglisi, C.; Carroccio, S.; Montaudo, G. *Macromolecules* **2002**, *35*, 4297–4305.
- (17) Carroccio, S.; Rizzarelli, P.; Gallet, G.; Karlsson, S. *Polymer* **2002**, *43*, 1081–1094.
- (18) Puglisi, C.; Carroccio, S.; Montaudo, G. *Polym. Degrad. Stab.* **2003**, *80*, 459–476.
- (19) Carroccio, S.; Puglisi, C.; Montaudo, G. *Macromolecules* **2003**, *36*, 7499–7507.
- (20) Carroccio, S.; Rizzarelli, P.; Puglisi, C.; Montaudo, G. *Macromolecules* **2004**, in press.
- (21) Chionna, D.; Puglisi, C.; Samperi, F.; Montaudo, G.; Turturro, A. *Macromol. Rapid Commun.* **2001**, *22*, 524–529.
- (22) Nyden, M. R.; Wallace, W. E.; Award, W. H. *Polym. Mater. Sci. Eng.* **2003**, *88*, 178–179.
- (23) Karlsson, S. *Polym. News* **2002**, *27*, 305–309.
- (24) Puglisi, C.; Samperi, F.; Di Giorgi, S.; Montaudo, G. *Polym. Degrad. Stab.* **2002**, *78*, 369–378.
- (25) Experiment performed in absence of oxygen (pure thermal degradation) did not show Norrish products. See ref 24.
- (26) Bandrup, J., Immergut, E. H., Eds. *Polymer Handbook*, 3rd ed.; John Wiley & Sons: New York, 1989.

MA049521N